УДК 539
P.A.C.S. 61.50.Ks
DOI 10.54708/26587572_2025_732277

EFFECT OF HIGH-PRESSURE TORSION PROCESS ON MECHANICAL PROPERTIES OF TC4-0.55Fe-0.08O ALLOY

Yihang He [1a], Yuecheng Dong [2], Igor Vasilevich Alexandrov [1]

[1] Ufa University of Science and Technology, 32 Zaki Validi st., 450076 Ufa, Republic of Bashkortostan, Russia
[2] Nanjing Tech University, 30 South Puzhu Road, 211816 Nanjing, Jiangsu Province, China
[a] zhouxujia1111@163.com

ABSTRACT

In the present study, the disc-shaped samples of TC4-0.55Fe-0.08O alloy were severely deformed by high-pressure torsion (HPT) under pressure of 6 GPa for 0.5, 1, 2 and 5 revolutions. The experimental results showed that the microhardness of TC4-0.55Fe-0.08O alloy treated with HPT was significantly increased by about 30% to 402 HV. The microhardness values were extremely heterogeneous along the diameter of the discs in the early stages of HPT and increased with the increase of the distance from the center to edges of the discs. Increasing the number of revolutions resulted in higher values and more uniform distribution of microhardness. The tensile properties of the HPT processed TC4-0.55Fe-0.08O alloy were investigated by unidirectional tensile testing at room temperature. It was found that the ultimate tensile strength of TC4-0.55Fe-0.08O alloy increased significantly with the increase in the number of HPT revolutions, from the initial 936 MPa to 1423 MPa after 2 revolutions, and then decreased slightly when the number of revolutions was increased to 5 revolutions. The elongation increased from the initial 11% to 13% after 1 revolution but then decreased sharply with the increase in the number of HPT revolutions. However, the ductility did not drop below 7%. The observations in this study indicated that the mechanical properties of TC4-0.55Fe-0.08O alloy can be improved as a result of HPT processing, which is of great significance for the practical production and application of TC4-0.55Fe-0.08O alloy.

KEYWORDS

Severe plastic deformation; high-pressure torsion; mechanical property; TC4-0.55Fe-0.08O alloy.

ВЛИЯНИЕ КВД НА МЕХАНИЧЕСКИЕ СВОЙСТВА СПЛАВА ТС4-0,55Fe-0,08O

Ихан Хэ [1a], Юэчэн Дун [2], Игорь Васильевич Александров [1]

[1] Уфимский университет науки и технологий, Россия, Республика Башкортостан, 450076 Уфа, ул. Заки Валиди, 32
[2] Нанкинский технологический университет, Китай, 211816 г. Нанкин, ул. Южная дорога Пужу, 30
[a] zhouxujia1111@163.com

АННОТАЦИЯ

В настоящем исследовании образцы в форме дисков из сплава ТС4-0,55Fe-0,08O были сильно деформированы кручением под высоким давлением (КВД). Кручение проводилось под давлением 6 ГПа с разным числом оборотов (n = 0,5, 1, 2 и 5). Экспериментальные результаты показали, что микротвердость сплава ТС4-0,55Fe-0,08O, обработанного КВД, увеличилась примерно на 30% до 402 HV. Значения микротвердости были крайне неоднородны вдоль диаметра дисков на ранних стадиях КВД и увеличивались с увеличением расстояния от центра к краям дисков. Увеличение числа оборотов приводило к более высоким значениям и более равномерному распределению микротвердости. Механические свойства сплава ТС4-0,55Fe-0,08O, обработанного КВД, также были исследованы путем однонаправленного испытания на растяжение при комнатной температуре. Было обнаружено, что предел прочности на растяжение сплава ТС4-0,55Fe-0,08O значительно увеличился с увеличением числа оборотов НРТ, с начальных 936 МПа до 1423 МПа после 2 оборотов, а затем немного уменьшился при увеличении числа оборотов до 5. Относительное удлинение увеличилось с начальных 11% до 13% после 1 оборота, но затем, с увеличением числа оборотов, резко уменьшилось. Однако пластичность не упала ниже 7%. Наблюдения в этом исследовании показали, что механические свойства сплава ТС4-0,55Fe-0,08O могут быть улучшены в результате обработки НРТ, что имеет большое значение для практического производства и применения сплава ТС4-0,55Fe-0,08O.

КЛЮЧЕВЫЕ СЛОВА

Интенсивная пластическая деформация; кручение под высоким давлением; механические свойства; сплав ТС4-0,55Fe-0,08O.

Introduction

Titanium alloys are widely used in aerospace, marine engineering, energy and chemical, and biomedical applications due to their excellent specific strength, corrosion resistance, and biocompatibility [1–5]. However, such properties of titanium alloys as strength, plasticity, and fatigue life are often required to be enhanced further to meet the demands of extreme service environments. Traditional strengthening methods, such as heat treatment, cold deformation processing and surface strengthening, can improve the material properties, but it is usually difficult to improve simultaneously strength and plasticity. Treatment by these methods even may lead to material embrittlement [6, 7]. Therefore, more and more attention has been paid to the research and development of high-performance titanium alloys to further expand their applications in various fields.

The two most common methods to improve the strength of materials are alloying [8] and grain refinement strengthening [9]. Fe as a powerful eutectic β-stabilizing element is inexpensive and processable, and is therefore often added to titanium alloys to improve the strength and hardness of the material [10, 11]. It is well known that the high hydrostatic pressure generated by severe plastic deformation (SPD) is conducive to the refinement of grain structure, and grain refinement can greatly improve the mechanical properties of materials. There are many different techniques for severe plastic deformation, but two deformation methods that received the most attention are equal channel angular pressing (ECAP) [12, 13] and high pressure torsion (HPT) [14, 15]. For titanium alloys, HPT process can be carried out directly at room temperature, and the grain size of the material is smaller after HPT treatment than after ECAP [16].

HPT is a typical SPD technique, which is capable of introducing very high strains in the material, thus significantly refining the grains to the submicrometer or even nanometer scale

and introducing a large number of crystal lattice defects such as dislocations and twins [17, 18]. This microstructural evolution can significantly increase the strength and hardness of the material, and at the same time, through appropriate process regulation, it can also make the material maintain a certain degree of plasticity, which can break through the problem of inverse ratio of strength and plasticity in the traditional reinforcement methods. HPT process can be used to avoid macroscopic cracks by applying a torsional shear strain to the disc sample under high pressure (usually several GPa), so as to make the material deform in a large extent in the constraints of quasi-hydrostatic pressure. HPT process is suitable for the preparation of nanostructured states of a wide range of metals and alloys [19, 20].

In recent years, important progress has been made in the study of HPT of titanium alloys. For example, Zhang and colleagues [21] produced a fully lamellar microstructure of cold-rolled Ti-6Al-4V alloy after appropriate heat treatment, and then processed it by HPT with different numbers of revolutions at room temperature. It was found that HPT processing up to 20 and 30 revolutions produced significant grain refinement of the material, with grain sizes of 70 nm and 50 nm, respectively. Václavová and colleagues [22] treated the metastable β-Ti alloy Ti-15Mo with solid solution, subjected it to severe plastic deformation through HPT processing, and studied the changes in the microhardness and elastic constants of the samples. The study found that the microhardness of the samples after HPT treatment increased significantly, and the Young's modulus first increased in the initial stage of HPT deformation, and then decreased with further strain. Barjaktarević and colleagues [23] obtained ultrafine grained Ti-13Nb-13Zr alloy by HPT processing under applied pressure of 4.1 GPa, a rotational speed of 0.2 rpm, 5 revolutions at room temperature. Investigations of the changes in the microhardness and tensile properties of the samples revealed that HPT processing led to an increase in the microhardness of the alloy. After tensile testing, it was found that HPT processing led to an increase in the tensile strength along with a decrease in the ductility of the alloy.

Currently, there are fewer studies on HPT processing of Fe and O microalloyed TC4 (Ti-6Al-4V) alloy. The Fe element in TC4-0.55Fe-0.08O alloy is conducive to grain refinement and microstructural changes during HPT, and the addition of Fe also leads to an increase in the ductility and toughness of titanium alloys [24, 25]. O is one of the stabilizing elements of the α-phase, and the mechanical properties of titanium alloys can be strongly affected by the addition of oxygen. In addition to this, the O element in TC4 alloy also has a strong solid solution strengthening [26–29]. Carrying out HPT research, in-depth study of the change rule of mechanical properties of the alloy in HPT process is of great significance to the practical application of TC4-0.55Fe-0.08O alloy.

This study takes TC4-0.55Fe-0.08O alloy as the object, treats it through HPT processing, and systematically analyzes the influence of HPT processing on the microhardness distribution and room temperature tensile properties of the alloy to provide theoretical basis and process reference for the development of high-performance titanium alloy, and to provide new ideas for the design of toughening titanium alloy.

1. Experimental material and methods

1.1. Material and HPT processing.

The material used in this study was forged TC4-0.55Fe-0.08O alloy. Thin disc samples having diameter of 20 mm and thickness of 1.3 mm were cut from a bar by using wire cutting equipment. Solid solution and aging treatments were carried out on these disc samples in a vacuum arc melting furnace. The solid solution treatment was carried out at 900 °C for 1.5 hours. Then after air cooling the aging treatment was carried out at 530 °C for 4 hours with final air cooling. The solid solution and aging treatments were conducted with the

aim to fully eliminate the internal stresses of the samples and improve the strength and ductility of the materials, thus ensuring the normal conduct of HPT experiments [30, 31]. The solid solution and aged samples were ground to a final thickness of about 1 mm and then deformed by the HPT processing. The lower anvil seat rotated clockwise at a constant speed of 1 revolution per minute (rpm) at room temperature for 0.5, 1, 2, or 5 revolutions. The HPT processed disc samples were denoted as 0.5R-, 1R-, 2R-, and 5R-TC4-0.55Fe-0.08O alloy samples, respectively, corresponding to the to the number of HPT revolutions.

1.2. Vickers microhardness test.

The disc samples before and after the HPT processing were polished to make the sample surface mirror-like. The hardness value of the sample was measured using an HV-1000 hardness tester under the applied load of 500g. Holding time was set as 15 s. The measurements were completed in the center of the discs and then in 12 adjacent areas with equal spacing of 1.5 mm along the diameter of the samples. In order to reduce the error of the results of the experiments the measurements were also conducted at 4 points in each of 13 areas (including the central area) along the diameter. The average value of the measurement in five points was considered as the final result of the test point. A total of 65 points were tested for each specimen.

1.3. Room temperature tensile test.

Tensile specimens were cut from the disc samples before and after HPT processing. The total length of each specimen was 10 mm, the total width was 5 mm, the gauge length was 4 mm, the gauge width was 1 mm, and the thickness was 1 mm, as shown in Fig. 1 [32]. The gauge length section of the tensile specimens was sanded with 800 grit sandpaper. The specimens were stretched using INSTRON equipment at room temperature with a strain rate of . The corresponding tensile stresses of the specimens were recorded by the experimental equipment until fracture of the specimens occurred. The engineering stress-strain curves of the specimens were obtained from these data [33].

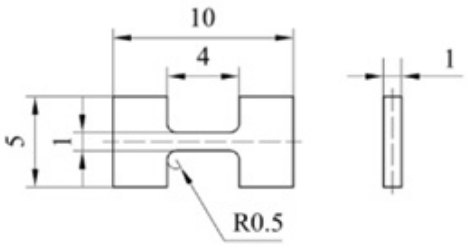

Fig. 1. The dimensions of tensile specimen (unit: mm) [30]

Рис. 1. Размеры образца для растяжения (ед. измерения: мм) [30]

1.4. Fracture morphology analysis.

The scanning electron microscopy method was used to observe the fracture morphology of the specimens after stretching at room temperature. The samples were cleaned using anhydrous ethanol and ultrasonic cleaner before the observation was carried out, and the specimens were blown dry with a high-pressure air gun and vacuum-encapsulated after the specimens were cleaned to avoid the influence of the specimen impurities on the observation results. As the TC4-0.55Fe-0.08O alloy has good electrical conductivity, the conductive adhesive was used to fixate the specimens before observation.

2. Results and discussion

2.1. Effect of HPT process on microhardness.

Fig. 2 shows the variation of microhardness of TC4-0.55Fe-0.08O alloy with the distance from the center of the sample. The experimental results show that microhardness of the samples before HPT processing is relatively uniform, with an average microhardness value of 308 HV. As a result of 0.5 revolutions of torsion, the microhardness increases rapidly, with

the hardness at the edge of the samples being 376 HV and the hardness at the center being 345 HV. The hardness values of the centers and edges increase slightly being measured after 1 and 2 revolutions of torsion. 5 revolutions of HPT resulted in a significant increase of the hardness at the center and edge of the sample. The hardness value at the center is about 393 HV, and the hardness at the edge reaches 402 HV. The hardness in the center of the HPT dics is lower than at the edges, but with the increase of the number of HPT revolutions, the microhardness along the diameter becomes more uniform.

Davidian and colleagues [34] showed that as the amount of high-pressure torsional stress increases, the content of ω phase also increases until saturation. Based on that the following conclusions can be drawn. When the samples were subjected to HPT at pressure of 6 GPa, the phase transition from α-phase to ω-phase occurs, and the microhardness increases with the increase of the content of ω-phase until the ω-phase reaches saturation. After 5 revolutions of HPT treatment, the ω phase of the sample tends to be saturated, and the hardness value is shown to be uniform.

From Fig. 2, it can be clearly seen that compared with the sample without HPT treatment, the microhardness of the sample after HPT treatment increases with the increase of the number of HPT revolutions. The increase in the number of revolutions results in the increase of the accumulated strain. The increase in accumulated strain results in the grain refinement and dislocation density increase during the HPT treatment of the alloy. The accumulated strain is higher near the edges of the samples. It results in smaller grain size and more high dislocation density near the edges of the samples. That is why the microhardness of the samples in early stages of HPT processing is extremely heterogeneous in the diameter direction, with the curve as a whole showing a V-shape. The increase in the number of revolutions results in the vortex nature of material flow. So, the microstructure and microhardness of the disks become more uniform.

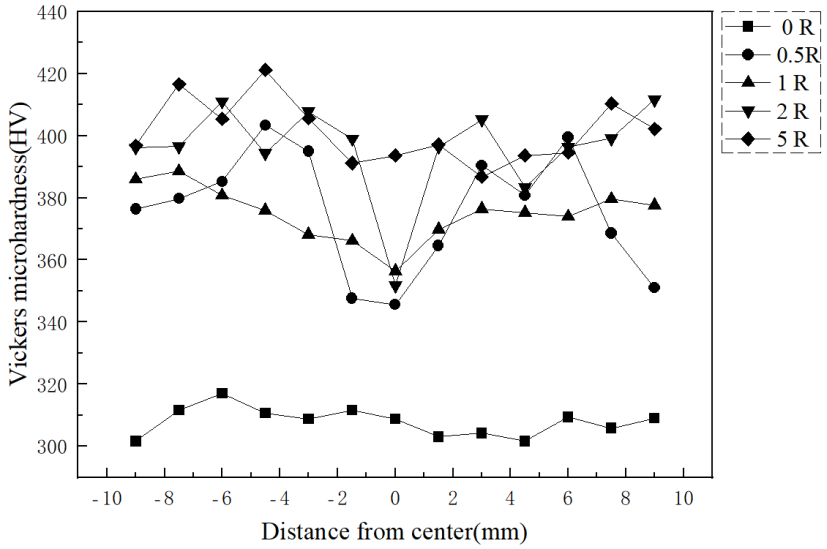

Fig. 2. The microhardness distribution along the diameter of the discs

Рис. 2. Распределение микротвердости вдоль диаметров дисков

2.2. Effect of HPT processing on room temperature tensile property.

Fig. 3 shows the true stress-strain curves at room temperature for TC4-0.55Fe-0.08O alloy with different numbers of HPT revolutions. The specific room temperature tensile experimental data are statistically presented in Table 1, which shows that the ultimate tensile strength of the initial sample is 936 MPa and the elongation is about 11%. After HPT processing, the ultimate tensile strength of the sample increases significantly, and it is 1368 MPa when the number of HPT revolutions is 0.5. It reaches the highest value, which is 1423 MPa, when the number of HPT revolutions is 2. The ultimate tensile strength of the sample decreases slightly to 1308 MPa when the number of HPT revolutions continues to increase to 5 revolutions. It is easy to find that the strength of the sample was increased by 52% by HPT processing at room temperature. The elongation of the samples also slightly increases after HPT processing, which is about 12% at 0.5 revolutions of deformation and reaches a maximum of 13% at 1 revolution of torsional deformation. However, the elongation decreases sharply when the number of HPT revolutions continues to increase to 2 and 5 revolutions.

It was found that when the TC4-0.55Fe-0.08O alloy is subjected to HPT processing, the tensile strength of the material increases significantly. This can be explained by the evolution of the phase composition, grain size refinement, and the dislocation density increase of the sample due to the HPT process. Increase in the number of HPT revolutions results in the higher content of the ω-phase, the higher grain refinement, and the higher dislocation density. As a result, the strength increases. The strength and plasticity of the sample decreases after 5 revolutions of deformation treatment, which can be explained by the change of ω phase content [34]. After 5 revolutions of HPT treatment, the relative content of the ω phase increases and tends to saturate, and the saturation of the ω phase leads to a drastic increase in the density of the phase interface. The difference in the elastic modulus of the hard and brittle ω phase and the β matrix triggers a localized stress concentration under tensile loading, which induces the microcracks to nucleate preferentially at the interface, triggering brittle fracture, which results in the reduction of the strength and plasticity of the samples [35]. Nevertheless, the tensile strength of the samples does not decrease significantly, which is due to the fact that the grain size at 5 revolutions of HPT treatment is smaller than that at 2 revolutions of the treatment. In general, the smaller the grain size, the higher the strength. The situation indicated by the experimental results is in general agreement with that shown for several other different titanium alloys after high pressure torsion [36, 37].

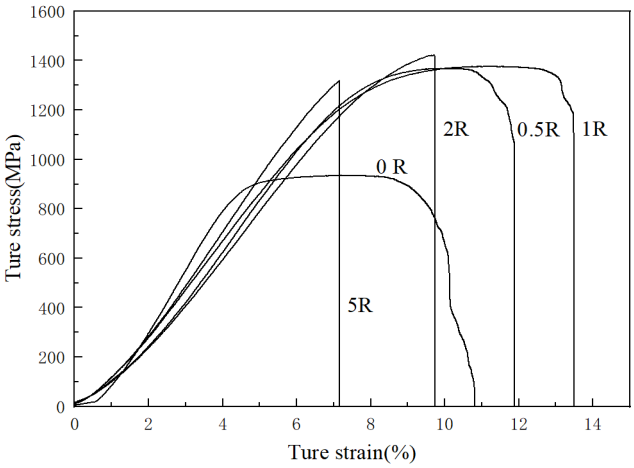

Fig. 3. True stress-strain curve for TC4-0.55Fe-0.08O alloy at room temperature

Рис. 3. Истинная кривая напряжения-деформации для сплава TC4-0,55Fe-0,08O при комнатной температуре

Table 1. Mechanical properties and related parameters of TC4-0.55Fe-0.08O alloy

Таблица 1. Механические свойства и соответствующие параметры сплава ТС4-0,55Fe-0,08O

Number of HPT revolutions / Число оборотов КВД	Strength (MPa) / Прочность (МПа)	Elongation (%) / Удлинение (%)
0	936	11
0.5	1368	12
1	1381	13
2	1423	10
5	1308	7

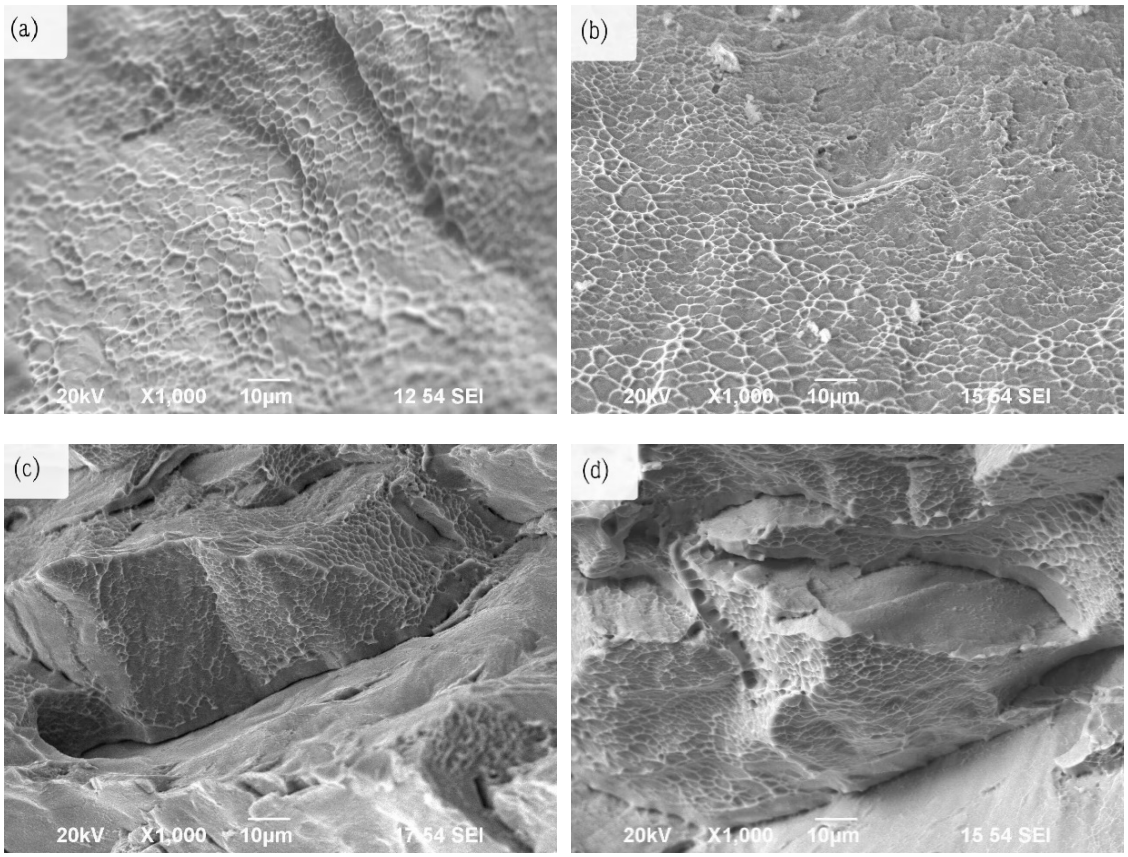

Fig. 4. Tensile fracture morphology of TC4-0.55Fe-0.08O alloy deformed at room temperature by HPT with:
a – 0.5R; b – 1R; c – 2R; d – 5R

Рис. 4. Морфология разрушения при растяжении сплава ТС4-0,55Fe-0,08O, деформированного при комнатной температуре методом КВД с:
a – 0,5R; b – 1R; c – 2R; d – 5R

2.3. Fracture morphology analysis.

The plasticity of the sample affects the morphology of the tensile fracture. High-plasticity materials experience significant plastic deformation before fracture, and the fracture surface usually has a dimple morphology. Low-plasticity materials show almost no plastic deformation before fracture, and the fracture surface shows cleavage or fracture along the grain [38]. The morphologies of the fracture surfaces of TC4-0.55Fe-0.08O alloy are shown in Fig. 4. The samples were subjected to tensile deformation at room temperature at the rate of 1×10^{-3} s^{-1}. HPT process was completed with 0.5, 1, 2, and 5 revolutions. The corresponding fracture surfaces are presented in Fig. 4, *a, b, c*, and *d*, respectively. Fracture surfaces presented in Fig. 4, *a* and *b* basically consist of dimples and tear ridges, which show a brittle fracture due to the relatively flat morphology and small, shallow dimples. This is because the initial samples were subjected to solid solution and aging treatment. At high temperature, with the prolongation of the holding time and the reduction of the cooling rate, the grains of the samples gradually grow, and the larger the size of the grains, the cracks are more likely to expand, resulting in the samples being susceptible to brittle fracture. In addition, when the samples are heat treated at high temperature, the samples absorb hydrogen, oxygen, nitrogen and other gases to form brittle compounds, which can also lead to material embrittlement [39]. As the number of HPT revolutions increases, dimples become larger and deeper. Fig. 4, *c* and *d* show more cleavage steps, dimples and some microvoids, and dimples tend to become smaller and shallower with the increase of the number of HPT revolutions. The fracture morphology shows that the plasticity of the samples firstly increases and then decreases, which is also consistent with the change rule of the stress-strain curve at room temperature.

Conclusions

In this study, TC4-0.55Fe-0.08O alloy was severely deformed by HPT process at room temperature under a pressure of 6GPa at a constant speed of 1 rpm. The corresponding mechanical properties of the deformed TC4-0.55Fe-0.08O samples were systematically investigated. Based on the experimental investigations, the following conclusions were drawn.

(1) The microhardness was significantly increased by HPT processing, reaching about 402 HV after 5 revolutions, with a corresponding increase of about 30% compared to the initial sample.

(2) The tensile strength increased significantly after HPT processing, reaching 1423 MPa after 2 revolutions, with a corresponding increase of about 52% compared to the initial sample. Then it slightly decreased.

(3) Tensile plasticity at the room temperature increased and then decreased sharply with the number of HPT revolutions.

(4) The evolution of the morphology of the fracture surfaces corresponds to an increase and then a decrease in plasticity with increasing number of revolutions.

(5) Based on the known literature data, the effect of HPT on the mechanical properties of the alloy can be explained by the competition between the phase transition, refinement of the grains, and the change in the dislocation density.

Acknowledgments / Благодарности

This research was funded by the Russian Science Foundation, grant No. 23-43-00041 (https://rscf.ru/project/23-43-00041/ accessed on 21 August 2024) and the National Natural Science Foundation of China, grant No. 52261135539.

Исследование выполнено при финансовой поддержке Российского научного фонда, грант № 23-43-00041 (https://rscf.ru/project/23-43-00041/ дата обращения: 21 августа 2024 г.), и Национального фонда естественных наук Китая, грант № 52261135539.

REFERENCES

1. Huang S., Zhao Q., Yang Z., et al. Strengthening effects of Al element on strength and impact toughness in titanium alloy // Journal of Materials Research and Technology. 2023. Vol. 26. P. 504–516.

2. Zhu C., Zhang X., Li C., et al. A strengthening strategy for metastable β titanium alloys: Synergy effect of primary α phase and β phase stability // Materials Science and Engineering: A. 2022. Vol. 852. Art. 143736.

3. Huang S., Zhao Q., Wu C., et al. Effects of β-stabilizer elements on microstructure formation and mechanical properties of titanium alloys // Journal of Alloys and Compounds. 2021. Vol. 876. Art. 160085.

4. Li C., Xin C., Wang Q., et al. A novel low-cost high-strength β titanium alloy: Microstructure evolution and mechanical behavior // Journal of Alloys and Compounds. 2023. Vol. 959. Art. 170497.

5. Su J., Jiang F., Tan C., et al. Additive manufacturing of fine-grained high-strength titanium alloy via multi-eutectoid elements alloying // Composites Part B: Engineering. 2023. Vol. 249. Art. 110399.

6. Healy C., Koch S., Siemers C., et al. Shear melting and high temperature embrittlement: theory and application to machining titanium // Physical Review Letters. 2015. Vol. 114(16). Art. 165501.

7. Ranjith Kumar G., Rajyalakshmi G., Swaroop S. A critical appraisal of laser peening and its impact on hydrogen embrittlement of titanium alloys // Proceedings of the Institution of Mechanical Engineers, Part B: Journal of Engineering Manufacture, 2019. Vol. 233(13). P. 2371-2398.

8. Su J., Jiang F., Tan C., et al. Additive manufacturing of fine-grained high-strength titanium alloy via multi-eutectoid elements alloying // Composites Part B: Engineering. 2023. Vol. 249. Art. 110399.

9. Balasubramanian N., Langdon T.G. The strength–grain size relationship in ultrafine-grained metals // Metallurgical and Materials Transactions A. 2016. Vol. 47. P. 5827–5838.

10. Abdalla A.O., Amrin A., Muhammad S., et al. Iron as a promising alloying element for the cost reduction of titanium alloys: A review // Applied Mechanics and Materials. 2017. Vol.864. P. 147–153.

11. Issariyapat A., Huang J., Kariya S., et al. Sustainable alloy design: Fe-enhanced Ti alloys for superior mechanical performance in additive manufacturing // Journal of Alloys and Compounds. 2025. Vol. 1010. Art. 177767.

12. Furukawa M., Horita Z., Nemoto M., et al. Processing of metals by equal-channel angular pressing // Journal of Materials Science. 2001. Vol. 36. P. 2835–2843.

13. Valiev R.Z, Langdon T.G. Principles of equal-channel angular pressing as a processing tool for grain refinement // Progress in Materials Science. 2006. Vol. 51(7). P. 881–981.

14. Zhilyaev A.P., Langdon T.G. Using high-pressure torsion for metal processing: Fundamentals and applications // Progress in Materials Science. 2008. Vol. 53(6). P. 893–979.

15. Zhilyaev A.P., Nurislamova G.V., Kim B.K., et al. Experimental parameters influencing grain refinement and microstructural evolution during high-pressure torsion // Acta Materialia. 2003. Vol. 51(3). P. 753–765.

16. Xu W., Edwards D.P., Wu X., et al. Promoting nano/ultrafine-duplex structure via accelerated α precipitation in a β-type titanium alloy severely deformed by high-pressure torsion // Scripta Materialia. 2013. Vol. 68(1). P. 67–70.

17. Pippan R. High-pressure torsion – features and applications In: Bulk Nanostructured Materials. Wiley-VCH Verlag GmbH & Co., 2009. P. 217–233.

18. Azzeddine H., Bradai D., Baudin T., et al. Texture evolution in high-pressure torsion processing // Progress in Materials Science. 2022. Vol. 125.Art. 100886.

19. Cao Y., Wang Y.B., Figueiredo R.B., et al. Three-dimensional shear-strain patterns induced by high-pressure torsion and their impact on hardness evolution // Acta Materialia. 2011. Vol. 59(10). P. 3903–3914.

20. Wei Q., Zhang H.T., Schuster B.E., et al. Microstructure and mechanical properties of super-strong nanocrystalline tungsten processed by high-pressure torsion // Acta Materialia. 2006. Vol. 54(15). P. 4079–4089.

21. Zhang W., Ding H., Pereira P.H.R., et al. Grain refinement and superplastic flow in a fully lamellar Ti-6Al-4V alloy processed by high-pressure torsion // Materials Science and Engineering: A. 2018. Vol. 732. P. 398–405.

22. Václavová K, Stráský J, Polyakova V, et al. Microhardness and microstructure evolution of ultra-fine grained Ti-15Mo and TIMETAL LCB alloys prepared by high pressure torsion // Materials Science and Engineering: A. 2017. Vol. 682. P. 220–228.

23. Barjaktarević D., Medjo B., Štefane P., et al. Tensile and corrosion properties of anodized ultrafine-grained Ti–13Nb–13Zr biomedical alloy obtained by high-pressure torsion // Metals and Materials International. 2021. Vol. 27. P. 3325–3341.

24. Meng L., Zhang Y., Zhao X., et al. The effects of Fe content on the microstructural evolution and tensile properties in Ti–6Al–4V-(2, 4) Fe alloys fabricated by thermomechanical powder consolidation // Materials Science and Engineering: A. 2021. Vol. 825. Art. 141877.

25. Gornakova A.S., Prokofjev S.I., Afonikova N.S., et al. Radial dependences of the phase composition, nanohardness, and Young's modulus for Ti–2 wt% Fe alloy after high-pressure torsion // Physical Mesomechanics. 2024. Vol. 27(6). P. 627–641.

26. Tang L., Fan J., Kou H., et al. Effect of oxygen variation on high cycle fatigue behavior of Ti-6Al-4V titanium alloy // Materials. 2020. Vol. 13(17). Art. 3858.

27. Nurly H.F., Ren D., Cai Y., et al. Effects of oxygen on microstructure and mechanical properties of selective laser melted Ti–6Al–4V annealed at different temperatures // Materials Science and Engineering: A. 2024. Vol. 894. Art. 146170.

28. Wu D., Zhang L., Liu L., et al. Effect of Fe content on microstructures and properties of Ti6Al4V alloy with combinatorial approach // Transactions of Nonferrous Metals Society of China. 2018. Vol. 28(9). P. 1714–1723.

29. Dai G., Niu J., Guo Y., et al. Microstructure evolution and grain refinement behavior during hot deformation of Fe micro-alloyed Ti-6Al-4V // Journal of Materials Research and Technology. 2021. Vol. 15. P. 1881–1895.

30. Li J., Zhang K., Hu R., et al. Design and microstructure-mechanical properties of a novel metastable β titanium alloy with excellent strength-plasticity matching // Journal of Materials Research and Technology. 2024. Vol. 28. P. 4177–4185.

31. Zhu Q., Yang X., Lan H., et al. Effect of solution treatments on microstructure and mechanical properties of Ti–6Al–4V alloy hot rolled sheet // Journal of Materials Research and Technology. 2023. Vol. 23. P. 5760–5771.

32. Wang Y., Jin Y., Guo Y., et al. Phase transformation and mechanical properties of nanocrystalline Ti–2Fe-0.1 B alloy processed by high pressure torsion // Journal of Materials Research and Technology. 2024. Vol. 31. P. 1853–1863.

33. Ballor J.A., Li T., Prima F., et al. A review of the metastable omega phase in beta titanium alloys: the phase transformation mechanisms and its effect on mechanical properties // International Materials Reviews. 2023. Vol. 68(1). P. 26–45.

34. Sun H., Liang Y., Li G., et al. Dislocation hardening and phase transformation-induced high ductility in Ti-6Al-4V with a heterogeneous martensitic microstructure under tensile load // Journal of Alloys and Compounds. 2021. Vol. 868. Art. 159155.

35. Davdian G.S., Gornakova A.S., Straumal B.B., et al. Effect of pre-annealing on the formation of the ω-phase in the Ti-2 wt% V alloy after high-pressure torsion // Journal of Materials Science. 2024. Vol. 59(14). P. 5771–5786.

36. Korneva A., Straumal B., Kilmametov A., et al. Phase transitions and mechanical behavior of Ti-3wt.% Nb alloy after high pressure torsion and low-temperature annealing // Materials Science and Engineering: A. 2022. Vol. 857. Art. 144096.

37. Ashida M., Hanai M., Chen P., et al. Developing microstructure and enhancing strength of Ti–6Al–7Nb alloy with heat treatment processed by high-pressure torsion // Materials Transactions. 2022. Vol. 63(6). P. 948–956.

38. Wang J., Zhao Y., Zhou W., et al. In-situ investigation on tensile deformation and fracture behaviors of a new metastable β titanium alloy // Materials Science and Engineering: A. 2021. Vol. 799. Art. 140187.

39. Wang Z., Yang S., Peng Z., et al. Effect of defects in laser selective melting of Ti-6Al-4V alloy on microstructure and mechanical properties after heat treatment // Optics & Laser Technology. 2022. Vol. 156. Art. 108522.